

Mechanical Stability, Magnetic and Electronic Properties of $\text{Sr}_{1-x}\text{Ba}_x\text{FeO}_3$: DFT+U Study

A. RAHMANI*, K. DRISS KHODJA AND B. AMRANI

*Centre de Microscopie Electronique, Département de Physique,
Université Oran 1, Oran, Algeria*

Received: 18.02.2020 & Accepted: 14.04.2020

Doi: [10.12693/APhysPolA.138.469](https://doi.org/10.12693/APhysPolA.138.469)

*e-mail: rahmani.ahlem@edu.univ-oran1.dz

We provide a thorough study of the structural, elastic, electronic and magnetic properties of the perovskite solid solution of $\text{Sr}_{1-x}\text{Ba}_x\text{FeO}_3$ within the framework of density functional theory (DFT), using the full-potential linearized augmented planewave plus local orbital FP-(L)APW+lo method. The found results provide predictions for the mixed perovskite solid solution $\text{Sr}_{1-x}\text{Ba}_x\text{FeO}_3$ ($x = 0.25, 0.5, 0.75$) for which no experimental or theoretical data are presently available. These compounds were supposed to have a cubic ferromagnetic structure for all x compositions. The GGA-PBE functional was chosen for the prediction of the structural properties, in particular the lattice parameter, the bulk modulus and its pressure derivative as well as the cohesive energy. For testing the mechanical stability of the $\text{Sr}_{1-x}\text{Ba}_x\text{FeO}_3$ compounds, we have studied their elastic constants and it has been found that these compounds are mechanically stable in their cubic perovskite structure. Several parameters related to the elastic constants have also been predicted, in particular Young's modulus, the shear modulus, Poisson's ratio, the anisotropic factor and the Debye temperature (θ_D). For the correct treatment of the high correlation of 3d-iron electrons, the Hubbard correction and TB-mBJ potential were added to the GGA-PBE functional for the analysis of the electronic and magnetic properties of $\text{Sr}_{1-x}\text{Ba}_x\text{FeO}_3$. It has been found that they are half-metals with a total magnetic moment of $\sim 4\mu_B$

topics: $\text{Sr}_{1-x}\text{Ba}_x\text{FeO}_3$, DFT, GGA+U, TB-mBJ potential, elastic constants, half-metallic

1. Introduction

Iron-based perovskites AFeO_3 ($\text{A} = \text{Ca}, \text{Sr}$ and Ba) belonging to the ferro-perovskites family represent a small class of compounds that contain an iron atom in a high-valence state of Fe^{4+} [1–8]. These compounds are of great interest in several application fields, particularly in spintronic technology [5, 9], thanks to their high spin-polarization of the conducting charge. Otherwise, compounds whose spin polarization near the Fermi level is 100% are called half-metals [10, 11].

In a ferro-perovskite, the introduction of an “A” element by substitution with a “B” element can improve its electronic and magnetic properties which motivated us to undertake a study with the aim to understand and predict the structural, electronic and magnetic behaviors of $\text{Ba}_x\text{Sr}_{1-x}\text{FeO}_3$. Matsui et al. have reported that a BaFeO_3 thin film has a pseudo-cubic perovskite structure with a cell parameter of 0.412 nm [12, 13]. On the other hand, a deposition of BaFeO_3 by a pulsed laser on SrTiO_3 substrates gave a stoichiometry of cubic BaFeO_3 thin films which are ferromagnetics insulating at room temperature [14, 15]. The magnetocaloric effect (MCE) of BaFeO_3 perovskite oxide has been investigated by M. Mizumaki et al. [16] and they found by the application of a small external magnetic

field that this compound is a ferromagnetic. Moreover, S. Chakraverty et al. [17] have reported that BaFeO_3 has an optical gap of 1.8 eV and a saturation magnetization with a Curie temperature of $3.2\mu_B$ /formula unit and 115 K.

SrFeO_3 is a metal with a cubic perovskite structure which also characterizes the helical spin order below $T_N = 134$ K [18, 19]. The application of a hydrostatic pressure on this compound promotes its transition between ferromagnetic and antiferromagnetic phases [20, 21]. Furthermore, and according to many theoretical results, SrFeO_3 is a ferromagnetic compound [22]. The DFT+U study of the high-pressure ferromagnetic phase transition of BaFeO_3 and SrFeO_3 under high pressure was the subject of Li et al.'s study [23], in which they found that the cause was the enhanced hybridization.

Cubic iron-based perovskites have a general formula of AFeO_3 whose space group is Pm-3m , in which atom positions of different atoms are: A (0.0; 0.0; 0.0), Fe (0.5; 0.5; 0.5) and O (0.0; 0.5; 0.5).

According to our knowledge, there are not only very few experimental but also no theoretical reports on the structural, electronic and magnetic behavior of $\text{Ba}_x\text{Sr}_{1-x}\text{FeO}_3$. Nevertheless, N. Hayashi et al. [24] have studied the structural and electronic properties of $\text{Ba}_x\text{Sr}_{1-x}\text{FeO}_3$ cubic

compounds by XRD, ND and magnetization measurements. This study was realized after they have successfully synthesized them.

In their paper, A. Iio et al. [25] have demonstrated that there is a possible application of these perovskites as a sensing electrode material (SE) and as potentiometric yttria-stabilized zirconia (YSZ)-based oxygen sensors for solid-state. Recently, K. Yoshii et al. [26] reported that $\text{Sr}_x\text{Ba}_{1-x}\text{FeO}_3$ perovskite is a candidate for magneto-caloric effect (MCE) material.

In the present theoretical work, we focused on the effect of Sr substitution on the structural, mechanical stability, electronic and magnetic behaviors of BaFeO_3 ferromagnetic cubic perovskite, namely, $\text{Sr}_x\text{Ba}_{1-x}\text{FeO}_3$ with $x = 0, 0.25, 0.5, 0.75, 1$.

This paper is organized as follows: in Sect. 2 we give a description of the computational method. In Sect. 3, we show all our results including structural, elastic, electronic and magnetic properties of $\text{Sr}_x\text{Ba}_{1-x}\text{FeO}_3$ ($x = 0, 0.25, 0.5, 0.75, 1.0$) with detailed discussion and interpretations. Finally, in Sect. 4, we summarize our conclusions.

2. Computational methods

Structural, elastic, electronic and magnetic properties of $\text{Sr}_x\text{Ba}_{1-x}\text{FeO}_3$ (with $x = 0, 0.25, 0.5, 0.75, 1$) were predicted using the first principles full-potential linearized augmented plane wave plus local orbital (FP-(L)APW+lo) method as implanted in WIEN2K package [27, 28]. The exchange-correlation potentials are treated using the generalized gradient approximation (GGA) of the Perdew, Burke, and Ernzerhof (PBE) functional [29].

The semilocal functionals (LDA or GGA) do not treat electronic and magnetic properties of solid materials with accuracy because they do not consider high correlations between the electrons of the heavy atoms. To resolve this problem, several theoretical models have been proposed. In this work, we have used the Hubbard correction term “U” which is added to the GGA-PBE semilocal functional with the already determined value of 3.1 eV [23, 30, 31].

To improve the prediction of the band-gap energies of $\text{Sr}_x\text{Ba}_{1-x}\text{FeO}_3$, the modified Becke-Johnson potential by Tran and Blaha (TB-mBJ) [32] has also been used. This choice is motivated by the success of this potential in the prediction of the band-gap energy of solid materials which gives very close values to those of the experimental. The muffin-tin radii for Ba/Sr, Fe and O are taken as 2.20, 1.80 and 1.75 a.u., respectively. The maximum value for partial waves inside the atomic sphere was $l_{max} = 10$. We have used a plane-wave cutoff $R_{MT}K_{max} = 9$ to expand the wave functions in the interstitial region that provides good convergence for the matrix size and 2500 k -points in the integration of the Brillouin zone for the convergence of energy eigenvalues. The calculations are obtained with a self-consistent convergence of total energy at 10^{-4} Ry.

3. Results and discussion

3.1 Structural properties

To predict the elastic, electronic and magnetic properties of $\text{Ba}_x\text{Sr}_{1-x}\text{FeO}_3$ compounds in the cubic structure, it is necessary to determine their structural properties first by determining their cell parameters (a_0) as well as the equilibrium volume (V_0), the bulk modulus (B) and total energy (E_0). This property also allows determining the most stable magnetic phase by predicting the total energy of the unit cell (the most stable phase is that of the lowest energy). All this information can be obtained by varying the volume as a function of the unit cell volume by fitting the curve with the Murnaghan equation [33]. We note here that according to our results, SrFeO_3 and BaFeO_3 are ferromagnetic compounds because their most stable energies correspond to that of the ferromagnetic phase, which confirms the previous experimental and theoretical results [14, 22, 23].

It is noted that the obtained values of the cell parameters and the bulk modulus for BaFeO_3 and SrFeO_3 are very close to those obtained previously. For all compositions ($x = 0, 0.25, 0.5, 0.75$ and 1), it is important to note the absence of any previous results for the heat of formation, as well as the derivative pressure of the bulk modulus. We also note the absence of all comparison results for $x = 0.25, 0.50$ and 0.75 .

Figure 1 shows the variation of the lattice constant and the bulk modulus as a function of the Sr composition, where the lattice constant falls with decreasing Sr-composition. This result can be explained by the fact that the atomic radius of Ba is greater than that of Sr-atom and the bonding nature has not changed (no changes in the interatomic distance). Otherwise, bulk modulus increases with concentration (x) which proves that the substitution of Sr-atom strengthens the hardness of the crystal system.

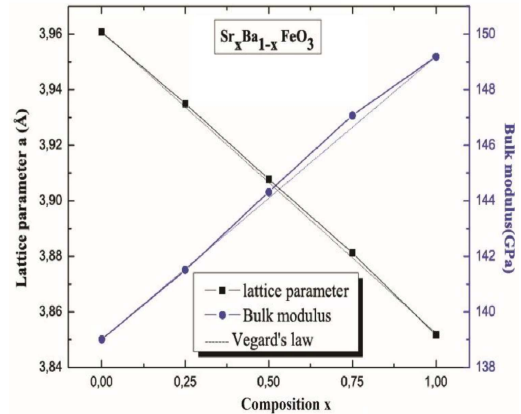


Fig. 1. Comparison between the lattice parameter and bulk modulus for $\text{Sr}_x\text{Ba}_{1-x}\text{FeO}_3$ alloys using Vegard's law as a function of composition x .

TABLE I

Calculated equilibrium lattice parameter a (Å), bulk modulus B (GPa), pressure derivative of the bulk modulus B' and the cohesive energy (eV/atom) of $\text{Sr}_x\text{Ba}_{1-x}\text{FeO}_3$ for various compositions, compared to some experimental [17, 22] and other theoretical [18, 23, 35, 36] works.

x	a	B	B'	E_{coh}	
0	3.96	139.01	4.79	-5.57	
	3.97 ^a				
	3.85 ^b	189.06 ^b			
	3.95 ^c				
	3.906 ^d				
0.25	3.94	141.5	4.44	-5.63	
0.5	3.91	144.32	5.02	-5.61	
0.75	3.88	147.07	5.27	-5.59	
1	3.85	149.2	4.83	-5.67	
	3.85 ^e				
	3.85 ^f				205.24 ^f
	3.79 ^d				

^aRef. [17], ^bRef. [23], ^cRef. [36], ^dRef. [35],

^eRef. [22], ^fRef. [18]

We also note that the variation of the cell-parameter as a function of x Sr-composition is almost linear and obeys Vegard's law [34], with marginal upward bowing parameters of -0.0116 Å. The variation of bulk modulus as a function of x Sr-composition has also upward bowing which is equal to -0.9 GPa. These values were obtained by a second order polynomial fitting of the calculated data. In fact, we find that the bulk modulus of BaFeO_3 is 6.8% higher than that of SrFeO_3 . This result suggests the existence of a significant downward bowing of the bulk modulus.

In Table I, we also presented the obtained values of the cohesive energy for all Sr-compositions. This quantity is defined as the difference between the total energy of isolated atoms that form the solid and its unit cell energy:

$$E_{\text{coh}}^{\text{Sr}_x\text{Ba}_{1-x}\text{FeO}_3} = E^{\text{Sr}_x\text{Ba}_{1-x}\text{FeO}_3} - (xE_{\text{Sr}} + (1-x)E_{\text{Ba}} + E_{\text{Fe}} + 3E_{\text{O}}). \quad (1)$$

3.2 Elastic properties

The study of the mechanical stability of a solid material is important and essential to start any other physical study. The elastic model achieves this objective by the prediction of the elastic constants C_{ij} . It also makes it possible to predict other related physical quantities for which their knowledge is very valuable, notably the Zener mechanical anisotropy, brittleness, ductility as well as the Debye temperature. It is well known that a cubic material has three elastic constants denoted as C_{11} , C_{12} and C_{44} , and to predict them, several theoretical models have been proposed. In this work, we

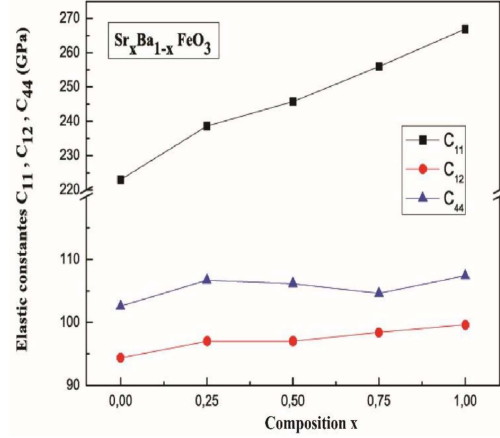


Fig. 2. Variation of the elastic constants of $\text{Sr}_x\text{Ba}_{1-x}\text{FeO}_3$ perovskites alloys as a function of composition x .

TABLE II

Calculated elastic constants C_{11} , C_{12} and C_{44} (GPa) of $\text{Sr}_x\text{Ba}_{1-x}\text{FeO}_3$ for various compositions.

x	C_{11}	C_{12}	C_{44}
0	223.04	94.37	102.58
	252.42 ^a	112.44 ^a	108.2 ^a
0.25	238.66	97.01	106.71
0.5	245.72	97.03	106.13
0.75	255.96	98.44	104.63
1	266.89	99.66	107.43
	291.04 ^a	118.43 ^a	114.82 ^a

^aRef. [35]

used the theoretical model, implanted in an IRelast package [37, 38], which has already been tested on a large number of materials and proved its effectiveness [39, 40]. The theoretical background of this method is explained in detail in [37–39].

All of the obtained results of $\text{Sr}_x\text{Ba}_{1-x}\text{FeO}_3$ elastic constants are grouped in Table II. We note that for all the studied materials, the elastic constants satisfy the stability criteria given by [41]: $C_{11} - C_{12} > 0$, $C_{11} > 0$, $C_{44} > 0$, $C_{11} + 2C_{12} > 0$, $C_{12} < B < C_{11}$ which means that these materials are mechanically stable in the cubic structural phase. Figure 2 represents the elastic constants variation of $\text{Sr}_x\text{Ba}_{1-x}\text{FeO}_3$ from which it is concluded that they increase linearly with the increase of the composition x of Sr atom.

The determination of the elastic constants allows the determination of other related mechanical and thermodynamic quantities such as the Zener anisotropy factor A , the shear modulus G , Young's modulus E , Poisson's ratio ν and the Debye temperature. Their relations are given as:

$$A = \frac{2C_{44}}{C_{11} - C_{12}}, \quad (2)$$

$$G = \frac{1}{5}(C_{11} - C_{12} + 3C_{44}), \quad (3)$$

$$E = \frac{9BG}{3B + G}, \quad (4)$$

$$v = \frac{3B - E}{6B}. \quad (5)$$

A value of the Zener anisotropy factor, which is close to unity, indicates the isotropy of a solid material while any far value indicates its anisotropy. The obtained values of the anisotropy factor for all studied materials (Table III) are higher than unity which indicates the anisotropic character of the studied compounds.

The shear modulus G , Young's modulus E and Poisson's ratio ν are important physical quantities that can inform us about the behavior of materials under the effect of external strains. The shear modulus can inform us about the resistive behavior of a material under the effect of external strains while Young's modulus E represents the relation between the external applied strains and the deformation of the material. Their values for $\text{Sr}_x\text{Ba}_{1-x}\text{FeO}_3$ are grouped in Table III. The absence of any previous results is noted.

Pugh's empirical relation (B/G ratio) [42] makes it possible to predict the brittleness or the ductility of a solid material by analyzing the value of B/G ratio, where a greater value than the limit value equal to 1.75 indicates the ductility of a solid material and a lower value indicates its brittleness. This calculated ratio is smaller than the limit value for all our results which means that $\text{Sr}_x\text{Ba}_{1-x}\text{FeO}_3$ are brittle materials.

The knowledge of the elastic constants makes it possible to determine a thermodynamic quantity of a great importance, namely the Debye temperature θ_D . Its determination allows the knowledge of other related thermodynamic quantities such as specific heat and melting temperature. It can be estimated by the following relation [43]:

$$\theta_D = \frac{hv_m}{k_B} \left(\frac{3n}{4\pi} \frac{N_A \rho}{M} \right)^{1/3}, \quad (6)$$

where h is Planck's constant, k_B is Boltzmann's constant, n is the number of atoms per formula unit, N_A is Avogadro's number, ρ is the density, M is the molecular mass per formula unit and v_m is the average wave velocity that can be determined by the following relation [44]:

$$v_m = 3^{1/3} \left(\frac{2}{v_l^3} + \frac{1}{v_t^3} \right)^{-1/3} \quad (7)$$

where v_l is the longitudinal elastic wave velocity and v_t is the transverse elastic wave velocity. They can be determined by the following relations [45]:

$$v_t = \sqrt{\frac{G}{\rho}}, \quad v_l = \sqrt{\frac{3B + 4G}{3\rho}}. \quad (8)$$

According to Table IV, it should be noted that the Debye temperature grows with the increase of x composition. This is due to the increase of the average wave velocity.

TABLE III

The calculated shear modulus G (GPa), ratio of B/G , Young's modulus E (GPa), Poisson's ratio ε and the Zener anisotropy factor A of $\text{Sr}_x\text{Ba}_{1-x}\text{FeO}_3$ for various compositions.

x	G	B/G	E	ε	A
0	85.08	1.63	211.99	0.25	1.59
	91.17 ^a	1.74 ^a	229.65 ^a	0.26 ^a	1.55 ^a
0.25	90.54	1.56	223.88	0.24	1.51
0.5	92.03	1.57	227.68	0.24	1.43
0.75	93.38	1.57	231.20	0.24	1.33
1	97.17	1.54	239.52	0.23	1.28
102.41 ^a	1.72 ^a	257.32 ^a	0.26 ^a	1.33 ^a	

^aRef. [35]

TABLE IV

Calculated longitudinal, transverse and average elastic wave velocity v_l , v_t and v_m (m/s), and the Debye temperature θ_D (K) of $\text{Sr}_x\text{Ba}_{1-x}\text{FeO}_3$ for various compositions.

x	v_l	v_t	v_m	θ_D
0	6236.77	3633.27	4030.41	518.05
0.25	6519.24	3811.05	4226.29	546.78
0.5	6688.65	3909.99	4336.02	564.88
0.75	6896.78	4015.57	4454.71	584.33
1	7156.58	4179.08	4634.87	612.62

It is important to note that according to Tables II and III, the obtained results of the elastic constants and their related mechanical quantities are in good agreement with the previous works that are available [35].

3.3 Electronic and magnetic properties

The study of the electronic and magnetic properties of $\text{Sr}_{1-x}\text{Ba}_x\text{FeO}_3$ represents the main objective of our work because information about these behaviors is precious to the experimentalists in classifying these materials according to their electronic importance and to propose their possible applications.

The analysis of the band structure and density of states allows to obtain knowledge about any solid material and its classification. The application of the semilocal functional including GGA and LDA makes it possible to precisely identify the nature of the band-gap but the functionals largely underestimate its value as they do not treat with accuracy the systems possessing highly correlated electrons including iron-based materials such as in the case of $\text{Sr}_{1-x}\text{Ba}_x\text{FeO}_3$.

Several theoretical models have been proposed to solve the problem of the large underestimation of the band-gap value by the semilocal functional including the potential of Becke-Johnson modified by Tran and Blaha [32] which is a well-known model. For the treatment of the highly correlated system, the Hubbard correction made to the

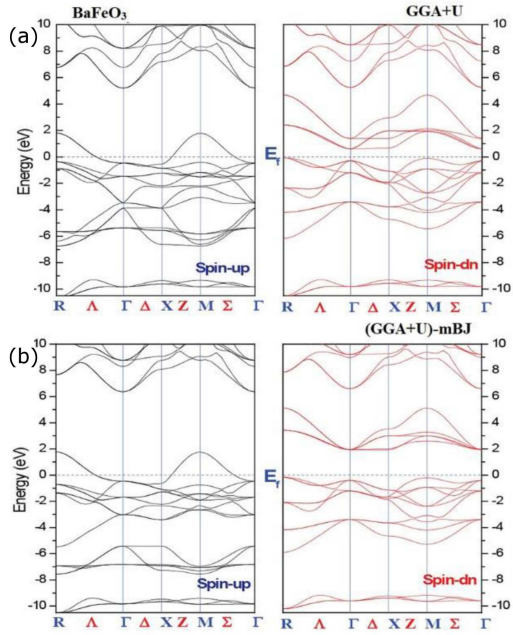


Fig. 3. Electronic band structure obtained using: (a) GGA+U, and (b) (GGA+U)-mBJ for BaFeO₃ perovskite.

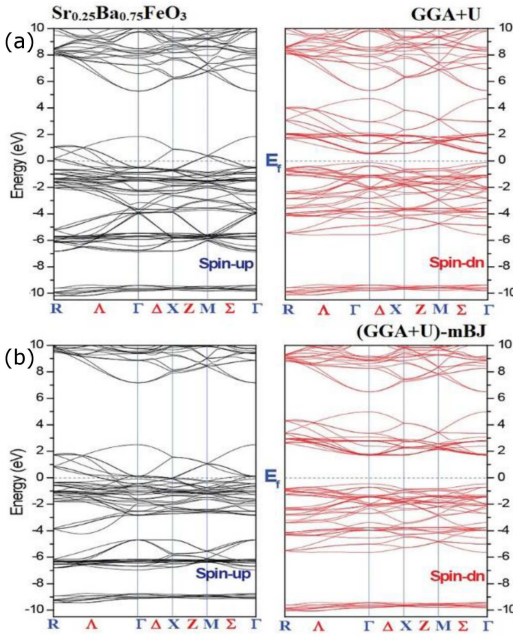


Fig. 4. Electronic band structure obtained using: (a) GGA+U, and (b) (GGA+U)-mBJ for Sr_{0.25}Ba_{0.75}FeO₃ perovskite.

semilocal functional represents a powerful method for this kind of study. In our work, we used the TB-mBJ potential [32] that was brought to GGA+U functional to calculate the band structures of Sr_{1-x}Ba_xFeO₃ which are illustrated in Figs. 3–7, and whose most ideal path (the path which makes it possible to scan the different directions of the first Brillouin zone for a cubic symmetry structure of Pm-3m space group) is given by the following high-symmetry points: R-Γ-X-M-Γ.

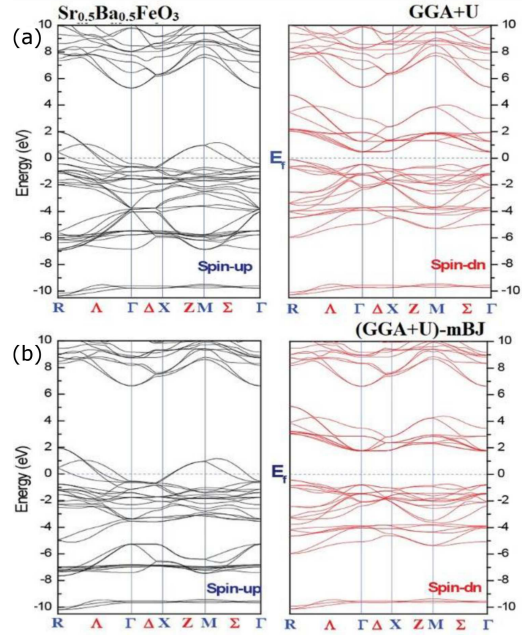


Fig. 5. Electronic band structure obtained using: (a) GGA+U, and (b) (GGA+U)-mBJ for Sr_{0.5}Ba_{0.5}FeO₃ perovskite.

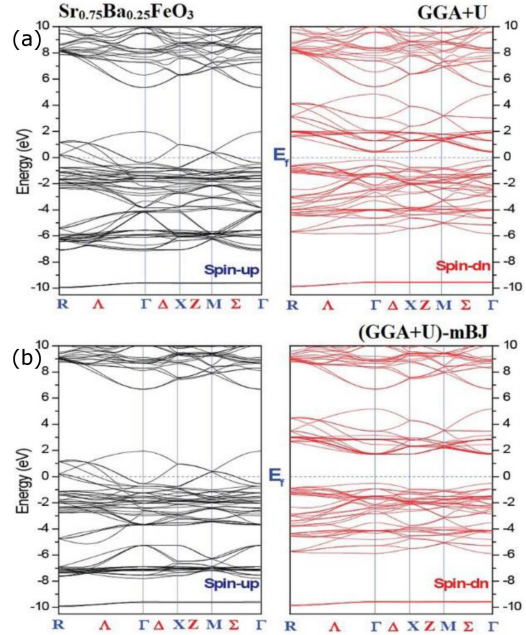


Fig. 6. Electronic band structure obtained using: (a) GGA+U, and (b) (GGA+U)-mBJ for Sr_{0.75}Ba_{0.25}FeO₃ perovskite.

According to the band structures of Sr_{1-x}Ba_xFeO₃, it is noted that the Fermi level passes through the middle of the valence band top for the spin-up states with the presence of a total band-gap (Spin-Up/Dn) which indicates a half-metallic behavior of these compounds. Note also that for BaFeO₃, SrFeO₃ and Sr_{0.5}Ba_{0.5}FeO₃, the fundamental band-gap is of indirect nature formed by the valence band top located at the R point of high symmetry and the conduction band

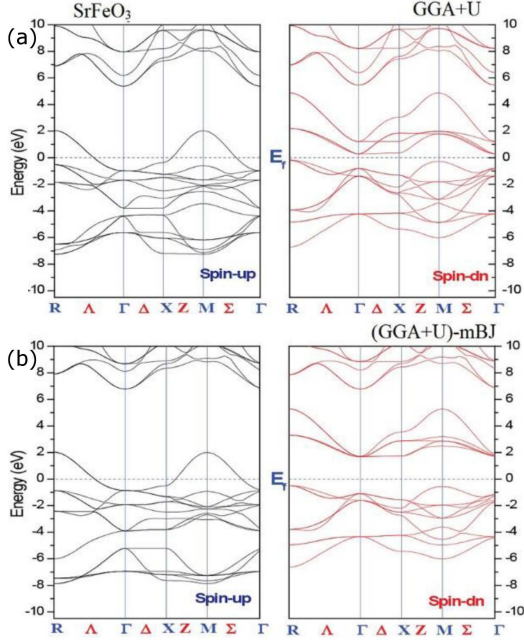


Fig. 7. Electronic band structure obtained using: (a) GGA+U, and (b) (GGA+U)-mBJ for SrFeO₃ perovskite.

bottom is located at Γ point of high symmetry. However, for the other studied materials in this work (Sr_{1-x}Ba_xFeO₃ with $x = 0.25$ and 0.75), the fundamental band-gap is of direct nature between the valence band top and the conduction band bottom which are located at the same Γ point of high symmetry.

The study of the spin polarization allows the prediction and confirmation of half-metallicity of Sr_{1-x}Ba_xFeO₃ which is identified by the following relation:

$$P = \frac{n(\uparrow) - n(\downarrow)}{n(\uparrow) + n(\downarrow)}, \quad (9)$$

where $n(\uparrow)$ and $n(\downarrow)$ are respectively the spin Up and Dn densities of states at the Fermi level. The spin polarizations of Sr_{1-x}Ba_xFeO₃ are 100% which confirms the half-metallicity behavior of these compounds. These results confirm previous work for the case of BaFeO₃ perovskite [23] and we observe that there is a lack of results for the other studied materials.

Table V summarizes all the obtained results for the band-gap values for different materials studied in this work. Note that for BaFeO₃, the band gap value estimated by GGA+U with the TB-mBJ potential is close to that found experimentally, unlike that obtained by GGA+U only. This remark allows us to predict that the obtained values with the TB-mBJ potential added to GGA+U will be close to the experimental values for other compounds once measured. These results make it possible to highlight the importance of these materials and allowed them to be proposed to experimentalists for possible spintronic applications.

TABLE V

Half metallic band gap energy (eV) with GGA+U and GGAmBJ+U of Sr_xBa_{1-x}FeO₃ for various compositions.

Compound	Method	EgHM
BaFeO ₃	GGA+U	0.68578 (R- Γ)
	mBJ	2.09064 (R- Γ)
	Exp	1.8 optical gap
Sr _{0.25} Ba _{0.75} FeO ₃	GGA+U	0.6525 (Γ - Γ)
	mBJ	2.16995 (Γ - Γ)
Sr _{0.5} Ba _{0.5} FeO ₃	GGA+U	0.63486 (R- Γ)
	mBJ	2.20296 (R- Γ)
Sr _{0.75} Ba _{0.25} FeO ₃	GGA+U	0.611191 (Γ - Γ)
	mBJ	2.21771 (Γ - Γ)
SrFeO ₃	GGA+U	0.54132 (R- Γ)
	mBJ	2.15921 (R- Γ)

TABLE VI

Calculated total and local magnetic moments (μ_B) of Sr_xBa_{1-x}FeO₃ for various compositions.

x	M_{Ba}	M_{Sr}	M_{Fe}	M_O	M_{int}	M_{tot}
0	0.009	–	3.591	0.080	0.162	4.001
0.25	0.011	0.007	3.543	0.086	0.173	3.992
0.5	0.010	0.006	3.539	0.092	0.174	4.005
0.75	0.012	0.007	3.527	0.096	0.178	4.012
1	–	0.005	3.542	0.089	0.191	4.005

The analysis of the density of states makes it possible to understand the formation of the bands and the determination of different states which form these bands. The valence band top and the conduction band bottom are the most important regions for a solid material because they are responsible for most of their physical properties. It can be observed from the Sr_{1-x}Ba_xFeO₃ curves of the density of states (Figs. 8–12) that the valence band top is dominated by a very high contribution of d states of iron in hybridization with p states of oxygen. The conduction band bottom of Sr_{1-x}Ba_xFeO₃ is dominated by d states of iron, strontium and barium.

Table VI gathers all the obtained results of the partial and total magnetic moments which are acquired by GGA+U approximation. We note that the total magnetic moment is calculated according to the number of each atom in the unit-cell [$M([x]Ba) + M([(1-x)]Sr) + M(Fe) + 3M(O) + M(int)$]. The values are very close to $4\mu_B$ due to a strong contribution of the Fe total moment (its value is $\sim 3.5\mu_B$ which is equivalent to 88.5% of the total magnetic moment) whose quantity in the unit cell does not change with the change of the x compositions between Ba and Sr, and for this reason, the magnetic moment changes slightly with the x change. The magnetic moment values of Fe are in agreement with the previously found values [16, 30]. These remarks make it possible to classify these compounds as promising materials for spintronic technology.

4. Conclusion

In this paper, we have studied the structural, elastic, electronic and magnetic properties of $\text{Sr}_x\text{Ba}_{1-x}\text{FeO}_3$ perovskite (with $x = 0, 0.25, 0.5, 0.75, 1$) using the full-potential linearized augmented planewave plus local orbital method (FP-(L)APW+lo) in the framework of the density functional theory as implemented in WIEN2K package.

The GGA-PBE exchange-correlations functional was used to study the structural properties such as the lattice constant, bulk modulus, its pressure derivatives and the cohesive energy. We have also predicted the elastic constants C_{11} , C_{12} and C_{44} , and their related parameters such as Young's modulus, the shear modulus and the Debye temperature θ_D . Our results need to be confirmed by future studies due to the lack of any experimental data. These compounds are mechanically stable because their elastic constants satisfy the elastic stability criteria. A linear variation of the lattice constant and the bulk modulus with x Sr-composition has been obtained. GGA+U within TB-mBJ potential were used for the treatment of the electronic and magnetic properties and we found that $\text{Sr}_x\text{Ba}_{1-x}\text{FeO}_3$ have a half-metallic behavior with a total magnetic moment of $4\mu_B$.

References

- [1] M. Takano, N. Nakanishi, Y. Takeda, S. Naka, T. Takada, *Mater. Res. Bull.* **12**, 923 (1977).
- [2] P.M. Woodward, D.E. Cox, E. Moshopoulou, A.W. Sleight, S. Morimoto, *Phys. Rev. B* **62**, 844 (2000).
- [3] T. Takeda, R. Kanno, Y. Kawamoto, M. Takano, S. Kawasaki, T. Kamiyama, F. Izumi, *Solid State Sci.* **2**, 673 (2000).
- [4] N. Hayashi, T. Terashima, M. Takano, *J. Mater. Chem.* **11**, 2235 (2001).
- [5] A.E. Bocquet, A.E. Bocquet, A. Fujimori, T. Mizokawa, T. Saitoh, H. Namatame, S. Suga, N. Kimizuka, Y. Takeda, M. Takano, *Phys. Rev. B* **45**, 1561 (1992).
- [6] M. Okube, Y. Furukawa, A. Yoshiasa, T. Hashimoto, M. Sugahara, A. Nakatsuka, *J. Phys. Conf. Ser.* **121**, 092004 (2008).
- [7] T. Tsuyama, T. Matsuda, S. Chakraverty, et al., *Phys. Rev. B* **91**, 115101 (2015).
- [8] J.B. MacChesney, J.F. Potter, R.C. Sherwood, H.J. Williams, *J. Chem. Phys.* **43**, 3317 (1965).
- [9] N.N. Oleynikov, V.A. Ketsko, *Russ. J. Inorg. Chem.* **49**, S1 (2004).
- [10] R.A. de Groot, F.M. Mueller, P.G. van Engen, K.H.J. Buschow, *Phys. Rev. Lett.* **50**, 2024 (1983).
- [11] W.E. Pickett, J.S. Moodera, *Phys. Today* **54**, 39 (2001).
- [12] T. Matsui, H. Tanaka, N. Fujimura, T. Ito, H. Mabuchi, K. Morii, *Appl. Phys. Lett.* **81**, 2764 (2002).
- [13] T. Matsui, E. Taketani, N. Fujimura, T. Ito, K. Morii, *J. Appl. Phys.* **93**, 6993 (2003).
- [14] N. Hayashi, T. Yamamoto, H. Kageyama, M. Nishi, Y. Watanabe, T. Kawakami, Y. Matsushita, A. Fujimori, M. Takano, *Angew. Chem. Int. Ed.* **50**, 12547 (2011).
- [15] C. Callender, D.P. Norton, *Appl. Phys. Lett.* **92**, 012514 (2008).
- [16] M. Mizumaki, K. Yoshii, N. Hayashi, T. Saito, Y. Shimakawa, M. Takano, *J. Appl. Phys.* **114**, 073901 (2013).
- [17] S. Chakraverty, T. Matsuda, N. Ogawa, H. Wadati, E. Ikenaga, M. Kawasaki, Y. Tokura, H.Y. Hwang, *Appl. Phys. Lett.* **103**, 142416 (2013).
- [18] T. Takeda, Y. Yamaguchi, H. Watanabe, *J. Phys. Soc. Jpn.* **33**, 967 (1972).
- [19] P. Adler, A. Lebon, V. Damljanovic, C. Ulrich, C. Bernhard, A.V. Boris, A. Maljuk, C.T. Lin, B. Keimer, *Phys. Rev. B* **73**, 094451 (2006).
- [20] S. Nasu, *Hyperfine Interact.* **128**, 101 (2000).
- [21] S. Nasu, T. Kawakami, S. Kawasaki, M. Takano, *Hyperfine Interact.* **144**, 119 (2002).
- [22] I.R. Shein, K.I. Shein, V.L. Kozhevnikov, A.L. Ivanovskii, *Phys. Solid State* **47**, 2082 (2005).
- [23] Z. Li, R. Laskowski, T. Iitaka, T. Tohyama, *Phys. Rev. B* **85**, 134419 (2012).
- [24] N. Hayashi, T. Yamamoto, A. Kitada, A. Matsuo, K. Kindo, J. Hester, H. Kageyama, M. Takano, *J. Phys. Soc. Jpn.* **82**, 113702 (2013).
- [25] A. Iio, H. Ikeda, S. Anggraini, N. Miura, *Solid State Ion.* **285**, 234 (2016).
- [26] K. Yoshii, N. Hayashi, M. Mizumaki, M. Takano, *AIP Adv.* **7**, 045117 (2017).
- [27] P. Blaha, K. Schwarz, G.K. Madsen, D. Kvasnicka, J. Luitz, "WIEN2K: An augmented plane wave + local orbitals program for calculating crystal properties", Technische Universität Wien, Vienna 2001.
- [28] O. Krogh Andersen, *Phys. Rev. B* **12**, 3060 (1975).
- [29] J.P. Perdew, K. Burke, M. Ernzerhof, *Phys. Rev. Lett.* **77**, 3865 (1996).
- [30] I.V. Maznichenko, S. Ostanin, L.V. Bekenov, V.N. Antonov, I. Mertig, A. Ernst, *Phys. Rev. B* **93**, 024411 (2016).

- [31] M. Mizumaki, H. Fujii, K. Yoshii, N. Hayashi, T. Saito, Y. Shimakawa, T. Uozumi, M. Takano, *Phys. Status Solidi C* **12**, 818 (2015).
- [32] D. Koller, F. Tran, P. Blaha, *Phys. Rev. B* **85**, 155109 (2012).
- [33] L. Vegard, *Z. Phys.* **5**, 17 (1921).
- [34] F.D. Murnaghan, *Proc. Natl. Acad. Sci. USA* **30**, 5390 (1944).
- [35] S. Maqsood, M. Rashid, F.U. Din, M. Bilal Saddique, A. Laref, *J. Electron. Mater.* **47**, 2032 (2018).
- [36] I. Cherair, N. Iles, L. Rabahi, A. Kellou, *Comput. Mater. Sci.* **126**, 491 (2017).
- [37] M. Jamal, S. Jalali Asadabadi, I. Ahmad, H.A. Rahnamaye Aliabad, *Comput. Mater. Sci.* **95**, 592 (2014).
- [38] M. Jamal, M. Bilal, I. Ahmad, S. Jalali Asadabadi, *J. Alloys Compd.* **735**, 569 (2018).
- [39] B. Sahli, H. Bouafia, B. Abidri, A. Bouaza, A. Akriche, S. Hiadsi, A. Abdellaoui, *Int. J. Mod. Phys. B* **30**, 1650230 (2016).
- [40] S. Hiadsi, H. Bouafia, B. Sahli, B. Abidri, A. Bouaza, A. Akriche, *Solid State Sci.* **58**, 1 (2016).
- [41] J.F. Nye, *Physical Properties of Crystals*, Oxford 1986.
- [42] S.F. Pugh, *Philos. Mag. J. Sci.* **45**, 823 (1954).
- [43] B. Mayer, H. Anton, E. Bott, M. Methfessel, J. Sticht, P.C. Schmidt, *Intermetallics* **11**, 23 (2003).
- [44] O.L. Anderson, *J. Phys. Chem. Solids* **24**, 909 (1963).
- [45] E. Schreibe, O.L. Anderson, N. Soga, *Elastic Constants and Their Measurements*, McGraw-Hill, New York 1973.